NUMERICAL EXPERIMENTS OF INDUCED EDDIES IN THE COASTAL OCEAN

Carlos A. A. Carbonel H.
Laboratório Nacional de Computação Científica
carbonel@lncc.br

Augusto C.N. Galeão
Laboratório Nacional de Computação Científica
acng@lncc.br

Abstract. *A gravity reduced finite element model in a coastal ocean is used for investigating the induced eddies due non uniform wind field. The hydrodynamical behavior is modeled by the motion and continuity equations; whereas the thermodynamical part is represented by the advection - diffusion transport equation for the temperature. It is a vertically integrated 1 ½ layer model. The equations apply only to the thin and warm oceanic surface layer. The deep layer is stipulated to be motionless and arbitrarily deep and separated from the upper layer by a density discontinuity. Cold deep water is carried across the interface from the lower into the upper layer. A Petrov-Galerkin formulation is considered to minimize effects of unresolved boundary layers improving the classical finite element Galerkin approach. The model uses continuous piecewise linear interpolation for the unknown variables on an unstructured mesh of triangular elements. Experiments are conducted to investigate the role of nonuniform winds; wind magnitude changes; and stratification, in the generation of eddies near the coast.*

Keywords*: Induced eddies; Finite elements; Petrov-Galerkin formulation; Hydrothermodynamics; Coastal ocean models;*

1. Introduction

A typical circulation pattern near ocean boundaries shows that upwelling-favorable winds force offshore drift at the ocean surface, leading to upwelling of cold subsurface water at the coast, and consequently the formation of offshore advection fronts. Nevertheless complex circulation patterns can also occur associated to several kinds of variability. A useful reference about these observational features was reported by Brink (1987), and also a collection of satellite photographs was reported by Narimousa and Maxworthy (1989).

The coastal regions are characterized by intense mesoscale activity, with generation and evolution of complex meanders, eddies and filaments along the coast. The processes responsible for the underlying dynamics of many of these features are not well understood (Strub et al. 1991), leaving us with an incomplete view of the controlling mechanism of large-scale and mesoscale variations of the physical properties.

Vortices are important features in flow research, and they are studied for theoretical and practical purposes. In fundamental flow research, the evolution of vortices is of great importance. Basically, a vortex could be defined as a swirling flow pattern, which will often behave as a coherent structure in time-dependent flows. A formal definition of a vortex cannot be easily given. Although in fluid dynamics research several criteria have been developed for their detection, the essential characteristics are hard to capture, and none of the existing criteria is entirely satisfactory (Sadarjoen, et aI., 2003).

Mesoscale eddies are not resolved in coarse resolution ocean models because they affect both mean momentum and scalars. Coarse resolution ocean codes (e.g., those used in climate studies, Griffies et aI., 2000) can only resolve the largest structures and leave the mesoscale eddies (50-100) km to be modeled.

Combining data from various sources (including satellite and in situ measurements) with numerical models of physics and biology can provide in a future a means for addressing questions about the physical and ecosystem processes.

The generation of eddies might be related to strong wind jets directed offshore for periods of 3-10 days as observed in the Gulfs of Tehuantepec and Papagayo (Mc Creary et al, 1989). Throughout the wind event, cyclonic and anticyclonic gyres spin up offshore on either side of the jet axis. Also the strengthening of coastal upwelling could be related to eddies generation as suggested by Schmidt et al. (1995). They studied a Brazil current frontal eddy near Victoria, using a hydrographic data set, drifting buoy observations and satellite imagery.

The rest of the paper is organized as follow. In section 2 the conservation equations and Petrov-Galerkin formulation are presented. The numerical experiments are showed in section 3

2. The model

2.1 The governing equations

A coastal ocean is defined in a domain $\Omega \subset R^2$. We consider land type boundary Γ_L and an ocean type boundary Γ_O, such that $\Gamma_O \cup \Gamma_L = \Gamma$ and $\Gamma_O \cap \Gamma_L = \Phi$. We use cartesian coordinates $(x,y) \in R^2$ oriented positively to the East and North respectively.

The vertical structure is composed by two layers. The upper layer of density ρ^u and thickness h, and an inert lower layer ρ^l where it is assumed that the horizontal pressure gradient is zero. In that way the faster barotropic mode is eliminated and just the first internal baroclinic mode is considered. The thermal structure is defined by the instant upper layer temperature T, and the lower layer temperature T^l.

As a constitutive state equation we assume the *ansatz*

$$\rho^u = \rho^l [1 - \alpha (T - T^l)], \tag{1}$$

where T is the actual temperature and α the thermal expansion coefficient. The influence of the salinity is not included, but there is no loss of generality, since an apparent temperature could be estimated modifying the constant α, to include the salinity effect (Hantel, 1971; Fofonoff, 1962).

For convenience, we define the variables

$$d = 2c\,,\ c = \sqrt{g\sigma h}\,,\ b = \frac{c^0 T}{T^u} \tag{2}$$

having the dimension of velocity. The parameter g represent the gravity acceleration, $\sigma = 1 - \rho^u/\rho^l$, and $c^0 = \sqrt{g\sigma H}$ is a referential celerity for the initial upper layer thickness H. T^u is the referential initial temperature in this layer.

Introducing a column array vector of unknown variables $V=(u,v,d,b)^T$, where u, v are the velocity components in the upper layer, the governing system of equations can be written as:

$$\underline{I}\frac{\partial V}{\partial t} + \underline{A}\frac{\partial V}{\partial x} + \underline{B}\frac{\partial V}{\partial y} + \underline{C}V + \underline{D}\left(\frac{\partial^2 V}{\partial x^2} + \frac{\partial^2 V}{\partial y^2}\right) + F = 0 \tag{3}$$

$$\underline{A} = \begin{pmatrix} u & 0 & c & s \\ 0 & u & 0 & 0 \\ c & 0 & u & 0 \\ 0 & 0 & 0 & u \end{pmatrix},\ \underline{B} = \begin{pmatrix} v & 0 & 0 & 0 \\ 0 & v & c & s \\ 0 & c & v & 0 \\ 0 & 0 & 0 & v \end{pmatrix},\ \underline{C} = \begin{pmatrix} 0 & -f & 0 & 0 \\ f & 0 & 0 & 0 \\ 0 & 0 & 0 & 0 \\ 0 & 0 & 0 & 0 \end{pmatrix},\ \underline{D} = \begin{pmatrix} -\vartheta & 0 & 0 & 0 \\ 0 & -\vartheta & 0 & 0 \\ 0 & 0 & 0 & 0 \\ 0 & 0 & 0 & -\vartheta_T \end{pmatrix},$$

$$F = \begin{pmatrix} -\tau_x / \rho^u h \\ -\tau_y / \rho^u h \\ -w_e g\sigma / c \\ (Q_I - Q)/h \end{pmatrix},\ V = \begin{pmatrix} u \\ v \\ d \\ b \end{pmatrix},\ \underline{I} = \begin{pmatrix} 1 & 0 & 0 & 0 \\ 0 & 1 & 0 & 0 \\ 0 & 0 & 1 & 0 \\ 0 & 0 & 0 & 1 \end{pmatrix},$$

The entrainment velocity w_e, is assumed to be $w_e = (H_e - h)^2 / t_e H_e$, where H_e and t_e represent respectively the depth and time scales of the entrainment-detrainment process, according to Mc Creary and Kundu (1988). The wind stress components are represented by $\tau_x = c_w \rho_{air} Wx / W /$, $\tau_y = c_w \rho_{air} Wy / W /$ where c_w is a constant and f is the Coriolis parameter that depends of the geographical coordinates. The eddy viscosity is represented by ϑ and ϑ_T is the thermal diffusivity. The function $s = gh\theta T^u / 2\bar{\mu} c^0$; $\bar{\mu} = \mu/(\mu - \sigma)$; $\mu = \rho^u/\rho^l$; $\sigma = 1 - \mu$.

The thermodynamic part of the model is driven by the surface heat flux Q which is the heat flux between the ocean and the atmosphere; and at the interface Q_I represent the gain or loss of heat across this interface, depending on the dynamical convergence or divergence of the flows ω in the upper layer and on the parameter $k_I = \omega H$ (Carbonel, 2003).

$$Q = (H/t_T)(T - T^l)/h \qquad Q_I = k_I(T - T^l)/h \tag{4}$$

On land type boundaries, we prescribe the non-slip conditions

$$u = v = 0 \tag{5}$$

and homogeneous boundary conditions are assumed for the upper thickness *h* and also for the temperature *T*.

For the open ocean boundary we prescribe a weakly reflective boundary condition is presented according to the characteristic method, in an axis (x_n) normal to the open boundary. Along the characteristics $dx_n/dt = u_n \pm c$ it is assumed that the *Riemann* invariant $R^{\pm} = u_n \pm d$ satisfy:

$$\frac{DR^{\pm}}{Dt} = 0 \tag{6}$$

where u_n represents the velocity component normal to the boundary. The weakly reflective conditions on the open boundary are defined by the in-going characteristic of the presented equations. (See Carbonel(2003) where the advantages of this kind of open boundaries modelling coastal upwelling were recently reported).

For the temperature at the open boundaries homogeneous condition are used.

Finally an appropriate initial state should be assumed in the domain Ω and at the boundary Γ:

$$u = u^o,\ v = v^o,\ h = h^o,\ T = T^o \text{ at } t = 0 \tag{7}$$

where u^o, v^o, h^o and T^o represent the initial velocity components, the thickness and the temperature respectively.

2.2 The Petrov-Galerkin formulation

To approximate the ocean problem previously presented we define a space-time finite element partition $\pi^{h,\Delta t}$, in which the time interval is partitioned into subintervals

$$I_n = t_{n+1} - t_n = \Delta t, \quad t \in [0, \Im] \tag{8}$$

where t_n, t_{n+1} belong to an ordered partition of time levels $0 = t_0 < \ldots t_n < t_{n+1} \ldots < t_F = \Im$.

For each *n* the space domain Ω is partitioned in N sub-domains Ω_e with boundary Γ_e, such that

$$\Omega_i \cap \Omega_j = \Phi \text{ for } i \neq j;\ i,j = 1,\ldots N \qquad \text{and} \qquad \bigcup_{e=1}^{N} \Omega_e = \Omega \tag{9}$$

As a result, for each *n=1,2...* the space-time domain of interest is the slab $S_n = \Omega \times I_n$ with boundary $\Gamma_n = \Gamma \times I_n$; the lateral surface of this "slab".

Under the above definitions we will assume that the finite element subspace of weighting functions is the set of continuous piecewise polynomials $\hat{V}^h$ in S_n, i.e.

$$\hat{U}_n^h \equiv \left\{ \hat{V}^h ; \hat{V}^h \in \left(C^0(S_n)\right)^4;\ \hat{V}^h\big|_{\Omega^e} \in \left(P^k(\Omega_e)\right)^4;\ \hat{V}^h\big|_{\Gamma_n} = 0 \right\} \tag{10}$$

Note that the previous definition implies that in the spatial domain each component of the vector $\hat{V}^h$ has C^o continuity; its restriction to a particular finite element Ω_e being a polynomial of degree less than or equal to *k*. Across the slab interfaces those components may be discontinuous. In this work, a continuous and linear interpolation in space and time will be adoptted.

Now let us introduce a vector $\overline{V}^h$ of prescribed boundary conditions on Γ_n. As a consequence, the set U_n^h of admissible trial functions will be:

$$U_n^h \equiv \left\{ V^h ; V^h \in \left(C^0(S_n)\right)^4;\ V^h\big|_{\Omega_e} \in \left(P^k(\Omega_e)\right)^4;\ V^h\big|_{\Gamma_n} = \overline{V}^h \right\} \tag{11}$$

For a general trial function V^h, the residual vector of the equation system (3) reads,

$$R^h = \underline{I}\frac{\partial V^h}{\partial t} + \underline{A}(V^h)\frac{\partial V^h}{\partial x} + \underline{B}(V^h)\frac{\partial V^h}{\partial y} + \underline{C}(V^h) + \underline{D}(\frac{\partial^2 V^h}{\partial x^2} + \frac{\partial^2 V^h}{\partial y^2}) + F \tag{12}$$

Then, we say that the space-time Petrov-Galerkin approximate solution for the hydro-thermodynamic problem is the vector $V^h \in U_n^h$, which satisfies $\forall\ \hat{V}^h \in \hat{U}_n^h$ the variational equation:

$$\int_{S_n} \hat{V}^h R^h \, d\Omega dt + \sum_{e=1}^{N} \int_{S_n^e} \overline{\Psi}_e \, G^h R^h \, d\Omega dt = 0 \tag{13}$$

where

$$G^h = \underline{I}\frac{\partial \hat{V}^h}{\partial t} + \underline{A}(V^h)\frac{\partial \hat{V}^h}{\partial x} + \underline{B}(V^h)\frac{\partial \hat{V}^h}{\partial y} \tag{14}$$

is a space-time operator, and

$$\overline{\Psi}_e = \tau \underline{I} \tag{15}$$

The algebraic equation system resulting from the PG weighting residual equation (13) will be solved using the direct method of Gauss.

3. Numerical Experiments

The numerical experiments performed to evaluate the coastal ocean dynamics assume that the fluid in the layers are initially at rest; and the following set of parameters is used: The time step is Δt = 21600sec. The densities of the upper and lower layer are ρ^u =1023.5 kgm^{-3} and ρ^l =1025.5 kgm^{-3}, ρ_{air}=1.175 kgm^{-3}. The initial upper layer thickness is H=50m. The entrainment depth H_e = 50m and the entrainment time scale t_e =0.5 days. The value of c_w = 1.8x10^{-3} is adopted. The initial upper temperature is T^u =26°C, and the lower layer temperature is T^l = 15^o C. The eddy viscosity ϑ is 400 m^{2}s and the difussivity is also ϑ_T =400 m^{2}s.

In the experiments, it is studied the physical behavior of a rectangular coastal ocean of 5°x 7° in the southern hemisphere. The coastal boundary is located in the western side, whereas the northern, eastward and southern boundary are open ocean boundaries. The northern boundary of the domain corresponds to the 18°S of latitude and the southern boundary is 25^{o}S.

In the nature, the wind stress causes the warmer surface water to drift away from the coast and allows cold bottom water to appear at the surface near the coast. The two masses of cold and warm water are separated by a front. During the migration the front become unstable as seen in many satellite infrared images showing filaments and plumes of cold water (Narimousa and Maxworthy, 1987). It is the objective of the present paper to explore the role of non uniform wind fields, magnitude change and stratification influence in the development of eddies.

3.1 Offshore Wind Patch

These kind of winds are observed in the nature, as for example is the mountain-pass jets that appears in the Gulfs of Tehuantepec and Papagayo for periods of 3-10 days (Mc Creary et aI, 1989), generating strong currents toward the jet axis and upwelling at the coast.

In the present study the offshore wind patch is acting on a western coastal region. The left panel of Figure 1 shows the horizontal structure of the wind stress which is 280km wide (meridional direction) and 400 km length (zonal direction). The wind velocity has maximal values of 15ms^{-1} at the coast, decreasing offshore.

The right panel of Figure 1 illustrates the response of the non-linear model to the offwind patch, showing the velocity and temperature fields at day 10. The circulation consists of two nearly symmetric gyres with a current flowing along the wind axis. The maximum speed of the offshore flow is 0.32ms^{-1}. The SST is cooled in a broad region induced by the offshore ageostrophic flow and associated to the clockwise gyre. The SST reaches a minimum of 22°C offshore due to Ekman pumping. The sheared flow field has a weak tendency to advect tongues of cold water around the anticlockwise gyre which a dispersion in offshore direction.

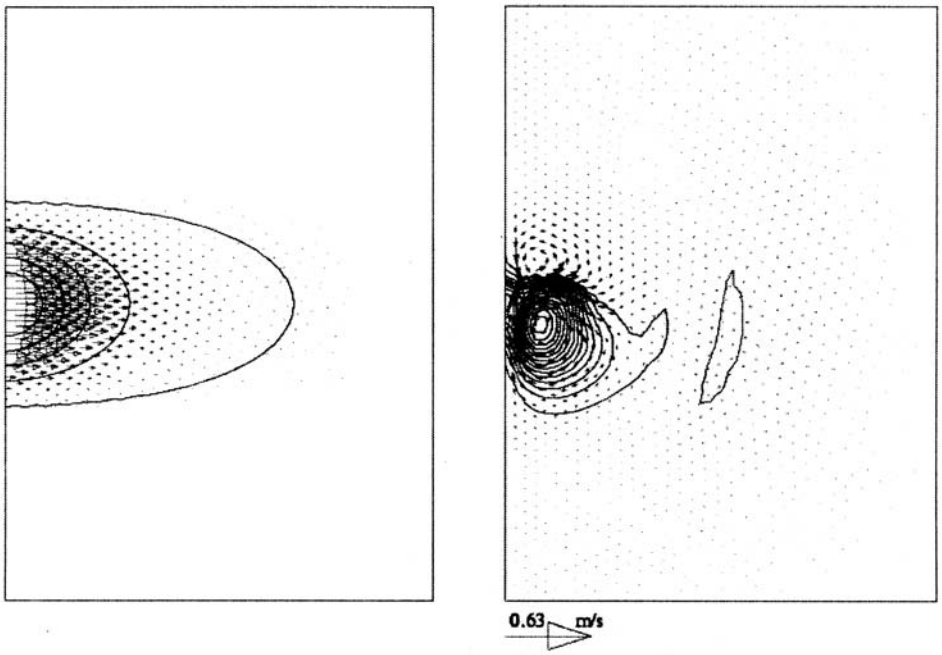

Figure 1. Offshore wind velocity field forcing (left panel), and the Velocity and SST fields at day 10 (right panel). Wind velocity contour is $3ms^{-1}$ with a maximum of $15ms^{-1}$. SST contour is *0.25°C* with a minimum of 22°C.

3.2 Southward wind patch

In the present case a southward wind patch is acting on the western coastal region. The left panel of Figure 2 shows the horizontal structure of the wind stress. The wind velocity has maximal values of $15ms^{-1}$ at the coast. The right panel of Figure 2 illustrates the model response to the southward patch, showing the velocity and temperature fields at day 10.

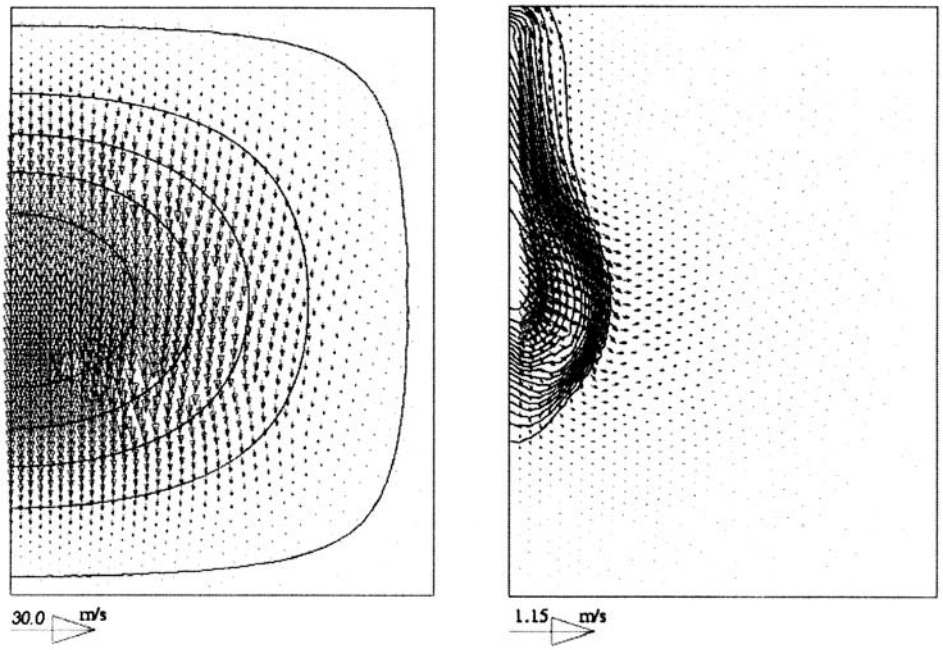

Figure 2. Southward wind field forcing (left panel). Velocity and SST fields at day 10 (right panel). The upwelling center is located at the coast. Wind velocity contour is $3ms^{-1}$. SST contour is 0.25*°C.*

The circulation consists of a coastal current with a maximum speed of $0.53ms^{-1}$. Due the Coriolis force coastal upwelling is generated at the coastline. The colder upwelling center increases their influence to the north. The SST is cooled in a broad region induced by upwelling reaching a minimum of 16°C in the upwelling center.

3.3 Relaxing of winds

Here, we present the results of established flows fields, when the wind changes their magnitude. The first case shown in Figure3 refers to the offshore wind patch forcing presented in section 3.2, when its action is stopped after 10 days. As observed in that figure, three days after the wind had been stopped, the dynamical and thermal patterns changes drastically as compared to those obtained at day 10.

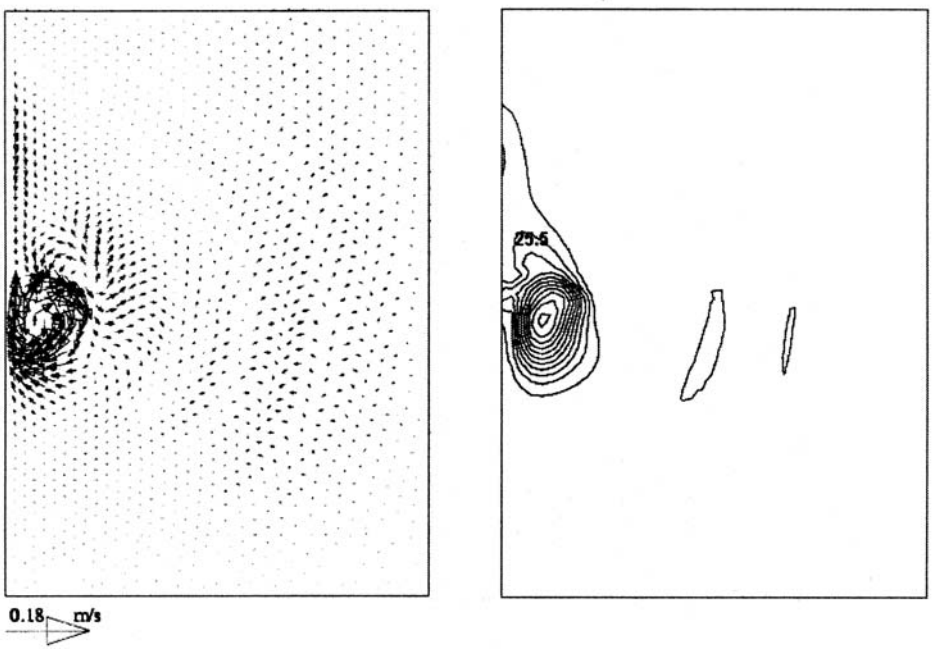

Figure 3. Relax of offshore wind patch forcing. Velocity field (left panel) and SST field (right panel) 2 days after the reductions of wind magnitude. SST contour is 0.25°C.

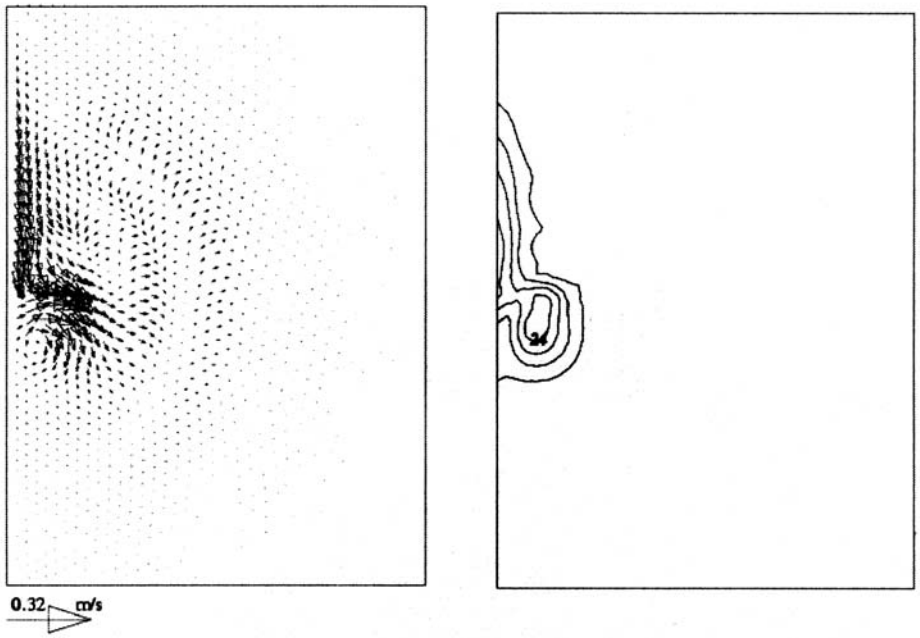

Figure 4. Relax of southward wind field forcing. Velocity field (left panel) and SST field (right panel) 2 days after the reductions of wind magnitude. SST contour is 0.25C.

The coastal waters begin a transient behavior to get an equilibrium state. The anticlockwise gyre disappears whereas the clockwise gyres remain but with smaller velocities. The SST shows the spreading of the colder

temperatures in northward direction. Also the temperature is reduced partially to around 23°C. Some amounts of water separated from the cold plume during the first 10 days are observed in the offshore side.

Next, we consider the case, where the southward wind patch forcing, presented in section 3.2, has its magnitude reduced to 50%, after the 10th day. The Figure 4 shows the velocity and SST field at day 12. The resulting SST pattern is warmer and the velocities are smaller than the previous one (Figure 2, right panel). As a consequence of the wind magnitude reduction, the cold upwelling plume pinch off in the southward sector of the cold plume, and a part is separated. The associated velocity field creates a clockwise gyre in the place where the separation of colder water takes place. This sector corresponds also to the downwind side of the southward patch. In the subsequent days, (not presented here) the coastal waters reaches a new equilibrium state with a cold plume, for which both the gyre and separation disappears.

3.4 Stratification influence

In the previous experiments the thermal structure and initial thickness used there, lead to a stratification characterized by: a wave celerity of order of 1.2 ms^{-1}; a Rossby radius *(c/f)* of 20 km and a Richardson number of 57 (considering a mean velocity of 0.15ms^{-1}). Now we increase the stratification changing the temperature difference between the two layer of the system choosing 29°C for the upper layer and 10°C for the lower layer. For these new thermal structure the wave celerity is now of order of 1.5 ms^{-1}, the Rossby radius *(c/f)* of 26 km and the Richardson number is 99. The other parameters remain the same and a run is performed for the offshore wind patch case. The results after 10 days is presented in Figure 5.

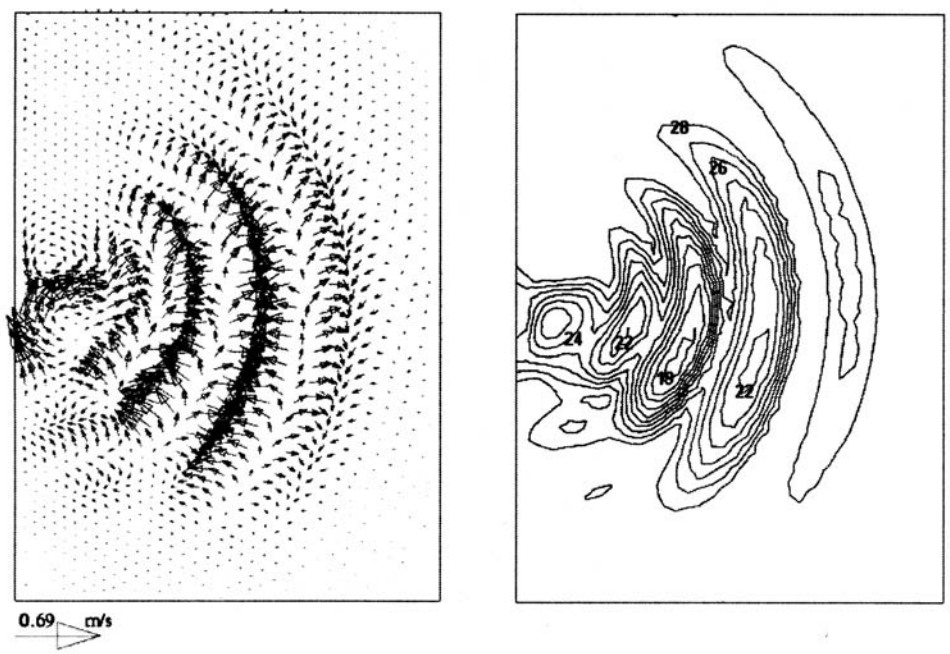

Figure 5. Solution for the southward wind field forcing for a increased stratification. Velocity field (left panel) and SST field (right panel) at day 10 days after the begin of wind setup. SST contour is 1°C.

In addition to the cool plume we can also observe that some additional cold cells are developped and they are going offshore. It is important to remark that the formed cells reach temperature values of minor magnitudes than those obtained for the cold cell near the coast, indicating that the associated circulation of the developed cells offshore drive an additional Ekman pumping.

It should also be noticed that the generated tongues of cold water pictured in Figure 5 (associated to the resulting shared current system in the eastward side of the original cold gyre), resulted from a stratification increasing for which the Richardson number almost double its value. Thought, this stratification change has a primarily influence on the pressure terms that depends on the parameter $\alpha\Delta T$. Apparently the baroclinic instability was the main reason. The generation of eddies, jets, squirts and cold filaments is a issue not well known in the oceanography.

4. Summary and conclusions

A finite element model, based on a Petrov Galerkin formulation in space and time, is used to describe the hydro-thermodynamical changes of wind forcing induced eddies in the surface layer of the coastal ocean. The ocean model is

a two dimensional gravity reduced layer system, that has an active layer overlaying a deep inert bed water, where the pressure gradient is set to zero. The Petrov-Galerkin formulation considered here, leads to stabilizing operators which effectively improve the classical Galerkin approaches. For the numerical experiments presented here, a constant free parameter was used to adjust the required stability.

The coastal ocean is forced by non-uniform wind fields. When a offshore wind patch is applied on a portion of the western coastal boundary, the resulting hydrothermodynamics at day 10 shows 2 gyres. When a southward wind patch flows an upwelling plume is generated.

For the offshore wind case, stopping the wind action, the cold plume weakens showing a spreading in northward direction. Moreover, increasing the stratification parameter clearly produces colder cells of water, that separate from the colder plume. In the southward wind case, for a 50% reduction in the wind action, the plume pinch off generating an eddy in the southward side and separating a colder water parcel.

The solutions show that wind patchs directed offshore, the change of magnitude of the wind field, and a higher stratification are some of the factors that induces eddies in the coastal ocean.

5. Acknowledgements

This research was partially supported by CNPq, FAPERJ/PRONEX 2003 no: E26/171.199/203 and MCT/PCI.

6. References

Di Lorenzo E., Miller AJ., Neilson D.J., Cornuelle B.C., Moisan J.R. 2004. Modelling observed California Current mesoscale eddies and the ecosystem response. INT. J. REMOTE SENSING, VOL. 25, NO. 7-8, 1307-1312.

Ari Sadarjoen Frits H. PostBing Ma David C. Banks Hans-Georg Pagendarm. Selective Visualization of Vortices in Hydrodynamic Flows.

Almeida R. C., Galeao A. c., Silva R.S., (1986) Adaptive Methods for the compressible Euler and Navier-Stokes Equations. Finite Elements in Fluids, 2, 337-346, Barcelona.

Bova, S.,W., Carey G.,F., (1995) An Entropy Variable Formulation and Petrov-Galerkin Methods for the Shallow Water Equations. In G. Carey, John Wiley, LondonEngland, Finite Element Modeling of Environmental Problems Surface and Subsurface Flow and Transport, 85-114. Brink K.H, 1987. Coastal Ocean Physical Processes. Rev. Geophysics, 25, 204-217.

Brooks AN., Hughes T. 1. (1982) Streamline Upwind Petrov-Galerkin Formulations for Convection-Dominated Flows with Particular Emphasis on the Incompressible Navier-Stokes Equations, Comput. Meths. Appl. Mech. Engrg. 32, 199-259.

Canuto V.M, Dubovikov M.S., 2005. Modeling Mesoscale Eddies. Ocean Modelling, 8, 1-30.

Carbonel H. C. A A and A C. N. Galeao (2004) Time Dependent Response of a Coastal Upwelling Region. A Finite Element Model. Journal of Coastal Research, SI 39. To be appear.

Carbonel, c., Galeao, A C. N. R. (2004) A Space-Time Petrov-Galerkin Model of the Upper Coastal Ocean Hydrodynamics in Limited Area Domain. Relatorio de Pesquisa e Desenvolvimento do LNCC, 10/2004.; ISSN 0101.6113.

Carbonel C. (2003) Modelling of Upwelling-Downwelling cycles caused by variable wind in a very sensitive coastal system. Continental Shelf Research, 23(16), 1559-1578.

Carbonel c., Galeao Ac., Loula A (2000) Characteristic Response of Petrov-Galerkin Formulations for the Shallow Water Wave Equations. Journal of the Brazilian Society of Mechanical Sciences, Vol. XXII,No 2, 231-247.

Fofonoff N. P. (1962) Dynamics of ocean currents. In: The Sea, Ed. M.N. Hill, New York, Voll, 323p.

Hantel M. (1971) Zum Einfluss des Entrainmentprozesses auf the Dynamik der Oberflachenschicht in einem tropisch subtropischen Ozean. Deutsche Hydrographische Zeitschrift. Jahrgang 24, 1971, Heft 3.

Hughes T., Mallet M. (1986) Finite Element Formulation for Computational Fluid Dynamics:III. The Generalized Streamline operator for Multidimensional Advective-Diffusive Systems. Comput. Meths. Appl. Mech. Engrg., Vol. 58, pp. 305-328.

Mc Creary J., Kundu P. (1988) A Numerical Investigation of the Somali Current during the Southwest Monsoon. Journal of Marine research, 46,25-58.

Mc Creary J., Lee H., Enfield D. (1989) The Response of the Coastal Ocean to Strong Offshore Winds: With Application to Circulation in the Gulfs ofTehuantepec and Papagayo. Journal of Marine research, 47,81-109.

Narimousa S. , Maxworthy T., 1989. Application of a Laboratory Model to the Interpretation of Coastal Upwelling. Dyn. Atmos Ocean, 13, 1-46.

Ribeiro F. L., Galeao A.c., Landau L., 1996. "A Space-Time Finite Element Formulation for the Shallow Water Equations". Development and Application of Computer Technics to Environmental Studies, Vol.VI, pp 403-414, Computational Mechanics Publication.

Shakib F. , (1988) "Finite Element Analysis of the Compressible Euler and Navier Stokes Equations". Phd. Thesis, Stanford University.